Particle acceleration during explosive reconnection due to tilt instabilities

B. Ripperda[1], R. Keppens[1], O. Porth[2]

[1] *Centre for mathematical Plasma Astrophysics, Department of Mathematics, KU Leuven, Celestijnenlaan 200B, B-3001 Leuven, Belgium*

[2] *Institut fur Theoretische Physik, Max-von-Laue-Str. 1, D-60438 Frankfurt, Germany*

Introduction

Reconnection is the change of topology of magnetic fields, in which dissipation effects, like Ohmic heating, are enhanced due to a strong localised current. The energy contained in the plasma can effectively be transferred by this mechanism into heat and particle acceleration. It is considered as the main mechanism for particle acceleration in magnetically dominated plasmas, for example in flares. This could explain flares observed in the solar corona [1] but also flare phenomena proposed in more extreme astrophysical environments like magnetars [2], pulsar winds [3] or black hole magnetospheres [4]. For non-relativistic global flows and within the fluid approximation, the evolution of such a system is described by the resistive magneto-hydrodynamics (MHD) equations. These equations are valid as long as the Alfvén velocity is much smaller than the speed of light, meaning that dominant MHD phenomena are occuring on Alfvénic timescales. The MHD model, being a single fluid description for low frequency phenomena in plasmas, cannot address particle acceleration in flares. To overcome this issue we focus on test particle dynamics at much smaller timescales, in quasi-static MHD snapshots.

Numerical setup

By means of two-and-a-half dimensional (2.5D) numerical simulations, we study the linear phase and the subsequent nonlinear evolution of the tilt instability within the framework of resistive MHD. In these MHD evolutions, we solve the relativistic guiding centre equations of motion to resolve particle position $\mathbf{R}$ and parallel momentum $\gamma m_0 v_\parallel$ [5]

$$\frac{d\mathbf{R}}{dt} = \frac{(\gamma v_\parallel)}{\gamma}\hat{\mathbf{b}} + \frac{\hat{\mathbf{b}}}{B\left(1-\frac{E_\perp^2}{B^2}\right)} \times \left\{ -\left(1-\frac{E_\perp^2}{B^2}\right) c\mathbf{E} + \frac{\mu_r c}{\gamma q}\nabla\left[B\left(1-\frac{E_\perp^2}{B^2}\right)^{1/2}\right] + \frac{v_\parallel E_\parallel}{c}\mathbf{u_E} \right.$$

$$\left. + \frac{c m_0 \gamma}{q}\left(v_\parallel^2\left(\hat{\mathbf{b}}\cdot\nabla\right)\hat{\mathbf{b}} + v_\parallel\left(\mathbf{u_E}\cdot\nabla\right)\hat{\mathbf{b}} + v_\parallel\left(\hat{\mathbf{b}}\cdot\nabla\right)\mathbf{u_E} + \left(\mathbf{u_E}\cdot\nabla\right)\mathbf{u_E}\right)\right\}, \quad (1)$$

$$\frac{d\left(m_0\gamma v_\parallel\right)}{dt} = m_0\gamma\mathbf{u_E}\cdot\left(v_\parallel^2\left(\hat{\mathbf{b}}\cdot\nabla\right)\hat{\mathbf{b}} + v_\parallel\left(\mathbf{u_E}\cdot\nabla\right)\hat{\mathbf{b}}\right) + qE_\parallel - \frac{\mu_r}{\gamma}\hat{\mathbf{b}}\cdot\nabla\left[B\left(1-\frac{E_\perp^2}{B^2}\right)^{1/2}\right], \quad (2)$$

$$\frac{d\left(m_0\gamma^{*2}v_\perp^{*2}/2B^*\right)}{dt} = \frac{d\mu_r^*}{dt} = 0. \tag{3}$$

with $\hat{\mathbf{b}}$ the unit vector in the direction of the magnetic field $\mathbf{B}$, E the amplitude of the electric field vector and $v_\parallel$ the component of the particle velocity vector parallel to $\hat{\mathbf{b}}$. The drift velocity, perpendicular to $\mathbf{B}$ is written as $\mathbf{u_E} = \frac{c\mathbf{E}\times\hat{\mathbf{b}}}{B}$ and $v_\perp^*$ is the perpendicular velocity the particle has, where we chose the frame of reference moving at $\mathbf{u_E}$. γ^* is the Lorentz factor in this frame of reference. The relativistic magnetic moment μ_r^* is an adiabatic invariant of the particle. The magnetic and electric fields are interpolated at the particle positions as input for equations (1-3). These equations are an approximation of the relativistic equations of motion for charged particles, neglecting the gyrating motion of a particle. The feedback of the particle motion on the magnetic fields is also neglected. This is valid as long as the particles gyroradius $R_L = \frac{\gamma m_0 v_\perp}{Bq}$ is much smaller than the typical cell size of the simulation and typical particle timescales are much smaller than Alfvénic timescales respectively. Both assumptions are perfectly valid in solar coronal conditions.

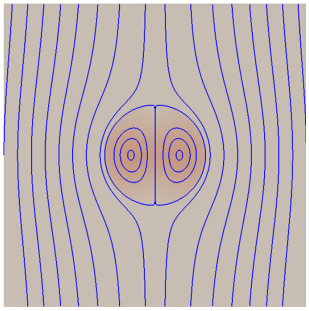

Figure 1: Total current distrbution at $t = 0$ including selected field lines. A linear colour scale is saturated to show values between $[0-50]$.

Starting from an ideal force-free MHD equilibrium of two anti-parallel, repelling current channels in a square region $[-3,3]\times[-3,3]$ in Cartesian coordinates (x,y), we describe the flux function

$$\psi_0(x,y) = \begin{cases} \frac{2}{j_0^1 J_0(j_0^1)} J_1(j_0^1 r)\cos(\theta) & \text{for } r < 1. \\ (r - \frac{1}{r})\cos(\theta) & \text{for } r \geq 1. \end{cases} \tag{4}$$

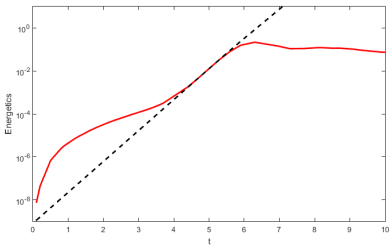

Figure 2: Kinetic energy density evolution integrated over a single current channel.

using $(r,\theta) = (\sqrt{x^2+y^2}, \arctan(y/x))$. J_n are the Bessel functions of the first kind and $j_0^1 \approx 3.831706$ is the first root of J_1. From the flux function, the magnetic field components of $\mathbf{B} = \nabla\psi_0 \times \hat{\mathbf{z}}$ in the (x,y) plane and the two anti-parallel currents $J_z = (\nabla\times\mathbf{B})_z = -\nabla^2\psi_0$ are found. In one half of the unit circle $J_z > 0$ and in the other half $J_z < 0$. We employ a force-free magnetic field with spatially varying, vertical component $B_z(x,y)$ such that the Lorentz force $\mathbf{J}\times\mathbf{B} = 0$

$$B_z(x,y) = \begin{cases} (j_0^1)(\psi_0(x,y)) & \text{for } r < 1. \\ 0 & \text{for } r \geq 1. \end{cases} \tag{5}$$

And a uniform plasma pressure $p_0 = 0.01/\Gamma$ with $\rho = 1$ and the ratio of specific heats $\Gamma = 5/3$ such that $\nabla p = 0$ and plasma $\beta = 0.04$ initially; The resistivity parameter is set to be uniform, finite and constant $\eta = 0.0001$ allowing for non-ideal reconnection effects to occur. All parameters are in dimensionless code units. This equilibrium is unstable to the ideal tilt instability in which the current channels start to rotate and separate on Alfvénic timescales [6]; [7].

Results

To trigger the tilt instability, the equilibrium is perturbed by an incompressible velocity field. Starting from equilibrium (see Fig. 1), both the MHD equations and the guiding centre equations of motion (1-3) are solved with the grid adaptive MPI-AMRVAC code [8], with a resolution of 2400×2400.

The tilt instability grows linearly, which can be seen by the kinetic energy evolution in a current channel in Fig. 2, with a growth rate of $\gamma_{tilt} = 1.6578$ as indicated by the dashed line. At $t \approx 6$ the nonlinear regime is reached, where resistive effects become important. In this phase secondary islands and nearly singular current sheets form and reconnection is likely to occur. A strong sign of magnetic reconnection is the presence of parallel electric fields, or more strictly $\mathbf{B} \times (\nabla \times E_{||}\mathbf{B}/B)\,/B \neq 0$ [9]. Based on this indicator, reconnection sites are the regions in between the current channels and at the boundaries of the current channels. In the far nonlinear regime, at $t = 8$, these regions show a strong localised current sheet and broken and reconnected field lines (Fig. 3).

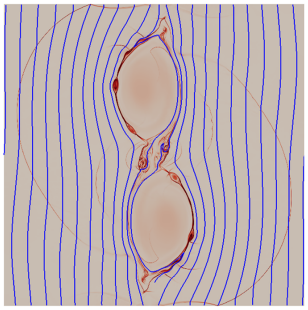

Figure 3: Total current distrbution at $t = 8$ including selected field lines. A linear colour scale is saturated to show values between $[0-50]$.

200.000 electrons are initiated with a Maxwellian velocity distribution for $v = \sqrt{(v_{||})^2 + (v_\perp)^2}$, corresponding to thermal velocity $v_{th} = \sqrt{(2k_BT/m_p \frac{\rho_0}{p_0})}$ of protons with rest mass $m_p = 1.6726 \cdot 10^{-24} g$ in a fluid of temperature around $T = 10^6 K$ in this MHD snapshot at $t = 8$. They are uniformly and randomly distributed at $x \in [-L/6, L/6]$ and $y \in [-L/2, L/2]$. All dimensionless MHD quantities are translated to cgs units and the typical system size is $L = 6 \cdot 10^6$ in both directions. The pitch angle $\alpha = \arctan(v_\perp^*/v_{||})$, indicates the angle between the velocity vector of the particle and the magnetic field direction. Initially the particles have a uniform pitch angle distribution $\alpha \in [-1.5, 1.5]$.

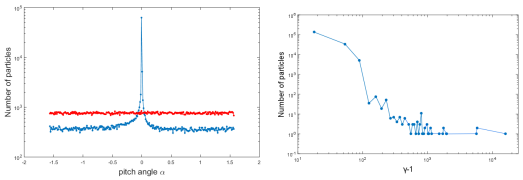

Figure 4: Left: Pitch angle distribution. Right: Lorentz factor distribution. Both for 200.000 electrons at $t = 8$.

Particles are accelerated within the current channels, which is a process that goes on indefinitely because of the translational invariance of the z-direction in 2.5D. This process gives the pitch angle distribution a large peak around $\alpha = 0$ This is a direct result of the small, but finite, resistivity that we adopt uniformly through the domain, leading to a parallel electric field component. For the MHD evolution this does not lead to any problems, but it dominates the particle acceleration because of the first term on the right hand side in equation 1 which can grow indefinitely (up to the speed of light) in the translationally invariant z-direction. Part of the distribution shows non-zero pitch angles (see left panel of Fig. 4, with the original distribution over-plotted in red) indicating that not all particles are accelerated by a parallel electric field. However, the main acceleration is in the direction parallel to the magnetic field. The total acceleration leads to a hardening of the kinetic energy $(\gamma - 1)m_0c^2$ spectrum, as observed in the Lorentz factor distribution, at $(\gamma - 1) \approx 10^2$ (right panel of Fig. 4). The distribution also shows a high energy tail at $(\gamma - 1) > 10^3$, developing from an initial Maxwellian distribution, again due to indefinite parallel acceleration.

Conclusions

Parallel acceleration and to a lesser extent, particle drifts, are an efficient way to obtain non-thermal distributions. Particles are artificially accelerated due to the translational invariance of the z-direction. This issue might be solved by introducing collisions moderating the parallel acceleration in the current channels. In future work, different equilibrium setups and plasma-β cases will be considered as well as 3D effects on particle acceleration and reconnection.

This research was supported by projects GOA/2015-014 (2014-2018 KU Leuven) and IAP P7/08 project CHARM. The simulations used the VSC (Flemish supercomputer center).

References

[1] S. Krucker, H. Hudson, L. Glesener et al., ApJ **714**, 1108 (2010)

[2] M. Lyutikov, MNRAS **346**, (2003)

[3] F. Michel, Rev. Mod. Phys, **54**, (1982)

[4] D. Wilkins, L. Gallo, D. Grupe, MNRAS **454**, (2015)

[5] T.G. Northrop, The Adiabatic Motion of Charged Particles (Interscience Publishers), (1963)

[6] R.L. Richard, R.D. Sydora and M. Ashour-Abdalla, PhFlB, **2**, 488 (1990)

[7] R. Keppens, O. Porth and C. Xia, ApJ, **795**, 1 (2014)

[8] O. Porth, C. Xia, T. Hendrix, S.P. Moschou and R. Keppens, ApJS, **214**, 4 (2014)

[9] G. Lapenta, S. Markidis, M.V. Goldman and D. Newman, Nature, **11**, 8 (2015)